DOI: 10.18721/JPM.13307
УДК 519.642; 550.388.2

AN ALGORITHM OF THE INITIAL APPROXIMATION FORMATION IN THE IONOSPHERIC TOMOGRAPHY PROBLEM WITH INTER-SATELLITE DATA REGISTRATION

P.N. Nikolaev

Samara National Research University, Samara, Russian Federation

In the paper, an original approach to the formation of the initial approximation in the ionospheric tomography problem with inter-satellite registration of total electron content is presented. The direct Radon transform of the electron density (ED)'s orbital profile is proposed to approximate using convolution of the function of latitudinal distribution of ED's maximum in the profile with the kernel function. This approximation makes it possible to estimate the latitude distribution of the ED maximum from the total electron content measurements by the deconvolution procedure. An analytical expression of the convolution kernel was obtained. Based on the proposed approach, two variants of formation of the initial approximation which used different prior information, namely, on the solar activity index and on the height of the ionization maximum in the profile, were considered. An accuracy of the mentioned formation was analyzed by the results of statistical simulation, and it was compared with the previously known approach where both the height of the ionization maximum in the profile and ED at this height were known.

Keywords: satellite monitoring, ionospheric tomography, initial estimation, statistical modeling

Citation: Nikolaev P.N., An algorithm of the initial approximation formation in the ionospheric tomography problem with inter-satellite data registration, St. Petersburg Polytechnical State University Journal. Physics and Mathematics. 13 (3) (2020) 80–92. DOI: 10.18721/JPM.13307

АЛГОРИТМ ФОРМИРОВАНИЯ НАЧАЛЬНОГО ПРИБЛИЖЕНИЯ В ЗАДАЧЕ ТОМОГРАФИИ ИОНОСФЕРЫ ПРИ МЕЖСПУТНИКОВОЙ СХЕМЕ РЕГИСТРАЦИИ ДАННЫХ

П.Н. Николаев

Самарский национальный исследовательский университет
имени академика С.П. Королева, г. Самара, Российская Федерация

В работе представлен оригинальный подход к формированию начального приближения в задаче томографии ионосферы при межспутниковой схеме регистрации данных полного электронного содержания (ПЭС). Предлагается аппроксимировать прямое преобразование Радона орбитального профиля электронной концентрации (ЭК) ионосферы сверткой функции широтного распределения максимума ЭК в профиле с функцией ядра. Такая аппроксимация позволяет оценить широтное распределение максимума ЭК по данным измерения ПЭС методом деконволюции. Получено аналитическое выражение функции ядра свертки. На основе предложенного подхода рассмотрены два варианта формирования начального приближения, использующие разную априорную информацию: об индексе солнечной активности и о высоте максимума ионизации в профиле. Проанализирована точность указанного

формирования по результатам статистического моделирования, проведено сравнение с известным подходом, когда известны как высота максимума ионизации в профиле, так и концентрация на этой высоте.

Ключевые слова: спутниковый мониторинг, томография ионосферы, начальное приближение; статистическое моделирование

Ссылка при цитировании: Николаев П.Н. Алгоритм формирования начального приближения в задаче томографии ионосферы при межспутниковой схеме регистрации данных // Научно-технические ведомости СПбГПУ. Физико-математические науки. 2020. Т. 3 № .13. С. 93–107. DOI: 10.18721/JPM.13307

Introduction

Methods for studying the ionosphere, aimed at remote sensing in a wide range of positions of transceiving systems, have seen increasing use in recent years. These systems make it possible to reconstruct the ionospheric structures based on computer tomography algorithms. Monitoring of the ionospheric electron density (ED) assesses the total electron content (TEC), which is a linear integral of the ED along the path of electromagnetic wave propagation, expressed in TECU units (Total Electron Content Units, 1 TECU = 10^{16} electrons·m^{-2}).

The linear integral of the distribution function $f(x,y)$ along the straight line located at a distance l from the origin and making an angle θ with the positive direction of the axis OX corresponds to the Radon transform at the point (l,θ):

$$\left[\tilde{R}f\right](l,\theta) = p(l,\theta) =$$

$$= \int_{-\infty}^{\infty}\int_{-\infty}^{\infty} f(x,y)\,\delta(x\cos\theta + y\sin\theta - l)\,dxdy.$$

The solution to the tomographic problem consists in finding the estimate $f^*(x,y)$ of the function $f(x,y)$ from a set of integral characteristics obtained from all possible angles, and assumes that the exact value of $p(l,\theta)$ is known for all l and θ.

The problem of radio tomography (RT) of the ionosphere is typically confined to solving systems of linear equations (SLE) [1]. In this case, the solution of the SLE is a complex computational problem, since the matrix of the SLE (projection operator) contains about 10^6–10^7 elements, even though it is sparse. An approach to solving the problem of ionospheric tomography was proposed in [2, 3] for an inter-satellite scheme for recording TEC data using a convolution algorithm.

The problem of ionospheric RT via satellites involves a small number of angles for obtaining the integral characteristic. Even though the positions of transceiver systems cover a wide range, whether it is a chain of ground receiving stations [4, 5] or proposals for space-based receivers and transmitters [6, 7], the obtained angles are still insufficient to satisfy the condition for the unique solution, and the inverse tomography problem is incorrect.

An initial approximation should be used to formulate the tomography problem correctly, corresponding to the distribution and values of the estimated parameters with some degree of confidence. For example, an IRI model (International Reference Ionosphere) and the Chapman distribution are used in [8–12] to construct the initial approximation for a chain of ground stations.

The initial approximation in [7, 13], where receivers and transmitters were used on the satellites of the ionospheric tomography system, was set in the entire reconstructed region to a constant value of $4\cdot10^{11}$ electrons·m^{-3}, which is the averaged value of the reference ED for all heights and latitudes in reconstructed region. However, because the ED of the equatorial ionosphere is higher than that of the mid-latitude and polar zones, and also because the system alternates between the illuminated and shadowed regions of the orbit due to the change between day and night, the accuracy with which such an initial approximation can be given is about 80–90%.

Ref. [13] compared the quality of ED reconstruction by a constellation of five satellites for an initial approximation given by a constant and for initial approximations obtained from the IRI-2007 ionospheric model [14], differing from the reference by 5, 10, 20 and 30% on average. The initial approximation based on the IRI ionospheric model yielded a better result compared with the initial approximation taken as constant.

In this study, we propose an original approach to rapidly formulating the initial

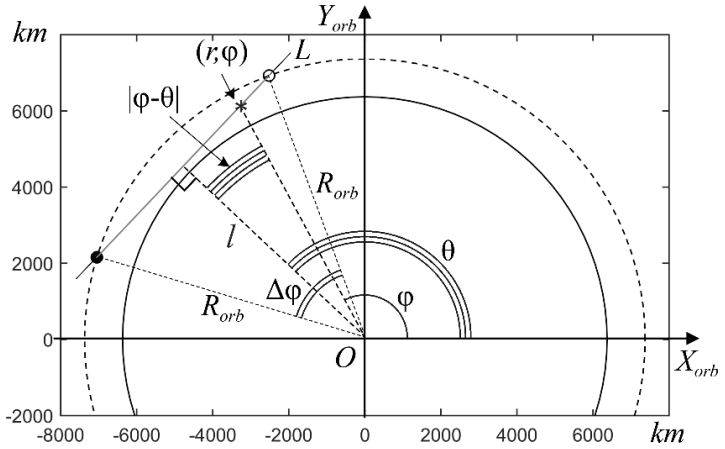

Fig. 1. Scheme of radio path with perigee altitude h_{track} = 225 km;
the dots indicate the location of two satellites in one circular orbit (dashed line)

approximation whose accuracy value is intermediate between the accuracy values provided by the approaches considered above.

The proposed approach has a number of advantages:

simpler mathematical implementation than the IRI-2007 model;

less input data required.

As a result, the satellites are supposed to have great autonomy (there is no need to transmit a large amount of input data to the satellite, such as ionospheric index, magnetic index, and solar activity indices).

This approach is applicable to obtaining integral characteristics by transceivers of a constellation of satellites located in the same orbital plane.

The accuracy of the initial approximation for the ionospheric ED profile is determined by numerical simulation, solving the forward and inverse problems.

The forward problem consists in obtaining the TEC for a given ED distribution in the orbital plane for a given radio path.

The inverse problem consists in reconstructing the ED distribution in the orbital plane from the available set of TEC measurements, with an initial approximation generated for this purpose. The generated initial approximation is compared with the given distribution.

The accuracy of the initial approximation was estimated in our study, as in [1, 7, 11], using the norms in the spaces l^2 and l^∞:

$$\delta\left(l^2\right)=\frac{\sqrt{\sum_i\left(F_i-\tilde{F}_i\right)^2}}{\sqrt{\sum_i F_i^2}},$$

$$\delta\left(l^\infty\right)=\frac{\max_i\left|F_i-\tilde{F}_i\right|}{\max_i\left|F_i\right|},$$

where F and $\tilde{F}$ are the model distribution and the generated initial approximation, respectively; i is the number of a pixel in the distribution.

The norm $\delta(l^2)$ is the root mean square establishing a large difference in the values of F and $\tilde{F}$ in a small region of the distribution. The norm $\delta(l^\infty)$ corresponds to the difference between F and $\tilde{F}$ in the worst case.

Problem statement

Consider two satellites located in the same circular orbit; one satellite serves as a transmitter, and the other as a receiver (Fig. 1). The satellites are located so that the perigee altitude of their radio path is below the maximum ED in the orbital profile. This number of satellites is sufficient to form an initial approximation by the proposed algorithm.

The height distribution of ED close to the Chapman distribution [9, 10] was taken as baseline:

$$N_e(h,N_m,H_m)=$$
$$=N_m\cdot\exp\left(1-\frac{h-H_m}{\sigma}-\exp\left(-\frac{h-H_m}{\sigma}\right)\right), \quad (1)$$

where N_m is the maximum value of ED N_e in the height profile; h is the altitude above sea level; H_m is the height of the maximum ED above sea level; σ is the scale parameter.

Algorithm for forming the initial approximation for the distribution of electron density in the ionosphere

Consider a circular polar orbit with an altitude of h_{orb} = 1000 km and an inclination of i = 90°. The satellites are located in orbit in such a way that the angular distance between them is equal to $\Delta\varphi$ = 54°, which corresponds to the satellites the farthest away from each other in orbit, from the constellation considered in [13] intended for solving the tomography problem in the altitude range of 200– 500 km. The chosen angular position of the satellites allows to form a radio path between them with a pericenter altitude h_{track} = 225 km. This radio path is certain to cross the ED maximum layer at two points; therefore, the TEC measured in this radio path is the largest among other TECs measured in the radio paths of the constellation [13].

The radio path between two satellites located in the same orbit (Fig. 1) is described in the polar coordinate system (CS) by the equation of the straight line

$$r(\varphi) = \frac{l}{\cos(\varphi - \theta)},$$

where l is the length of the perpendicular dropped to the straight radio path from the origin, $l = R_{\text{Earth}} + h_{track}$; θ is the the angle between the positive direction of the axis OX_{orb} and the direction of this perpendicular; R_{Earth} is the average radius of the Earth, R_{Earth} = 6371.136 km.

The height of the maximum ED H_m in the formula (1) depends on the latitude φ (this is due to the changing day and night conditions of the formation of the ionospheric profile), as well as on the zenith angle of the Sun [15]. To use expression (1) and carry out further analytical calculations for the segment of the orbit where the radio path is determined, we assumed that the height of the maximum ED H_m is the average in the segment $\Delta\varphi$ = 54°:

$$\langle H_m \rangle = \frac{1}{2\pi}\int_{\varphi_1}^{\varphi_2} H_m(\varphi)\, d\varphi,$$

where φ_1, φ_2 are the angular coordinates of the first and second satellite, respectively.

The measurements can cover more than 20° in latitude for RT using a chain of ground stations. Given this value of the latitudinal angular distance, it is acceptable to use the initial approximation (1) with a constant height of the ED maximum, as established in [11, 12]. Since the angular distance between two intersections of the ED maximum by the radio path was taken about 20° in this study, it seems reasonable to assume that the height of the ED maximum H_m is constant in the segment $\Delta\varphi$ = 54°.

Thus, the distribution of ED (1) in the orbital plane of the transmitter and receiver in the segment $\Delta\varphi$ is expressed as follows in the polar SC:

$$N_e(r,\varphi) = N_m(\varphi) \times \times \exp\left(1 - \frac{r - R_m}{\sigma} - \exp\left(-\frac{r - R_m}{\sigma}\right)\right), \quad (2)$$

where φ is the angular coordinate in the polar SC; $r = R_{\text{Earth}} + h$ is the radial coordinate in the polar CS; $Rm = R_{\text{Earth}} + \langle H_m \rangle$.

The linear integral from $N_e(r,\varphi)$ along the radio line L is curvilinear in the polar SC:

$$p(l,\theta) = \int_L N_e(r,\varphi)\, dl = \int_{\varphi_1}^{\varphi_2} N_e\left(r(\varphi),\varphi\right) \cdot \sqrt{r^2 + \left(\frac{dr}{d\varphi}\right)^2}\, d\varphi,$$

where the equation of the radio path for a small angle $\varphi - \theta$ has the form

$$r(\varphi) = \frac{l}{\cos(\varphi - \theta)} \approx l\left(1 + \frac{1}{2}(\varphi - \theta)^2\right).$$

Thus, $p(l,\theta)$ is written as the integral of the convolution for the function N_m and the kernel g (Fig. 2) with respect to the parameter θ:

$$p(l,\theta) = (N_m * g)(\theta) = \int_{\varphi_1}^{\varphi_2} N_m(\varphi) \cdot g(\varphi - \theta)\, d\varphi,$$

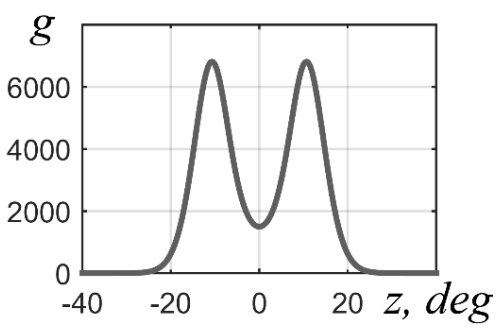

Fig. 2. Convolution kernel $g(z)$

where

$$g(z) = l \cdot \left(1 + z^2\right) \cdot$$
$$\cdot \exp\left(1 - \frac{1}{\sigma} \cdot (l - R_m) - \frac{l}{2\sigma} z^2 - \right.$$
$$\left. - \exp\left(-\frac{1}{\sigma} \cdot (l - R_m) - \frac{l}{2\sigma} z^2\right)\right).$$

The expression for $p(l,\theta)$ makes a transition to infinite limits with respect to the angle φ:

$$p(l,\theta) = \int_{-\infty}^{+\infty} N_m(\varphi) \cdot g(\varphi - \theta)\, d\varphi,$$

since $g(\varphi - \theta)$ decays exponentially for $\varphi \to \varphi_1$, φ_2 (Fig. 2).

Since the expression for the convolution integral is known, the latitudinal ED profile $N_m(\varphi)$ can be estimated using the deconvolution method [16]:

$$\hat{N}_m(\varphi) =$$
$$= F^{-1}\left(\frac{G^*(f)}{|G(f)|^2 + \alpha\left\langle |G(f)|^2 \right\rangle} \cdot P(f)\right) = (3)$$
$$= F^{-1}\left(W(f) \cdot P(f)\right) = (w * p)(\varphi),$$

where $G(f)$, $W(f)$, $P(f)$ are the Fourier images for g, w and p, respectively; $G^*(f)$ is the conjugate Fourier transform for g; α is the regularization parameter; $\langle |G(f)|^2 \rangle$ is the average value of the energy spectrum $G(f)$.

Substituting expression (3) into Eq. (2), the expression for modeling the initial approximation takes the form

$$N_e(h,\varphi) = (w * p)(\varphi) \cdot$$
$$\cdot \exp\left(1 - \frac{h - H_m}{\sigma} - \exp\left(-\frac{h - H_m}{\sigma}\right)\right). \quad (4)$$

The resulting expression is the product of the latitudinal ionospheric profile $(w \cdot p)(\varphi)$ and the height profile

$$\exp\left(1 - \frac{h - H_m}{\sigma} - \exp\left(-\frac{h - H_m}{\sigma}\right)\right),$$

from which it follows that the latitude and height profiles can be found separately.

If the latitudinal profile can be found by Eq. (3), then the height profile can be formed under different assumptions, which will affect the final accuracy of the initial approximation.

Thus, expression (4) can serve as a basis for formulating two versions of the algorithm for generating the initial ED approximation.

Version 1. The height is taken as an average over the orbit $H_m = \langle H_m \rangle$. Then,

$$N_e(h,\varphi) = (w * p)(\varphi) \cdot$$
$$\cdot \exp\left(1 - \frac{h - \langle H_m \rangle}{\sigma} - \exp\left(-\frac{h - \langle H_m \rangle}{\sigma}\right)\right). \quad (5)$$

Version 2. The height H_m is known a priori. Then,

$$N_e(h,\varphi) = (w * p)(\varphi) \cdot$$
$$\cdot \exp\left(1 - \frac{h - H_{m\,apr}}{\sigma} - \exp\left(-\frac{h - H_{m\,apr}}{\sigma}\right)\right). \quad (6)$$

The efficiency of the proposed versions can be estimated numerically by using the stochastic approach and comparing the result of the algorithm with the simulated distribution.

Results and discussion

Estimating the accuracy of the initial approximation based on the results of statistical modeling. Let us compare the two proposed versions for forming the initial approximation of the ionospheric ED profile in the plane of the satellite orbit with one known parameter. Three possible cases are possible here (cases *II* and *III* correspond to versions 1 and 2).

Case I. The initial approximation is formed by Eq. (1), when the parameters N_m and H_m are given a priori (this method was considered in [11, 12]);

Case II. The initial approximation is formed by Eq. (5), when $H_m = \langle H_m \rangle$;

Case III. The initial approximation is formed by Eq. (6), when H_m is known a priori.

We assessed the accuracy of all three cases of forming the initial approximation by statistical modeling of the ED distribution in the plane of the polar orbit (10,000 numerical experiments) for different indices of solar activity, months, Greenwich Mean Time, and geographic longitudes. Consider a circular polar orbit of two satellites with an altitude $h_{orb} = 1000$ km and an inclination $i = 90^\circ$. The angular distance between the satellites is considered to be constant, equal to $\Delta\varphi = 54^\circ$, which corresponds to the perigee altitude of their radio path $h_{track} = 200$ km. As the satellites were moving in orbit, the TEC was recorded every 0.5°.

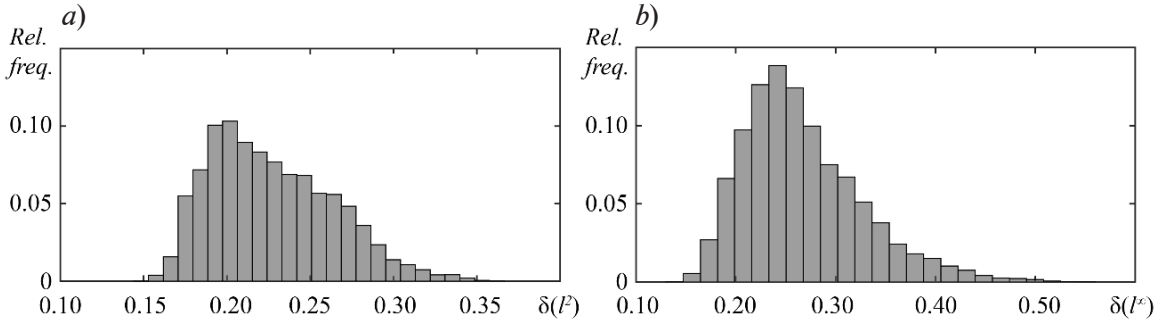

Fig. 3. Histograms of errors in forming the initial approximations by known parameters (case I) in metrics l^2 (*a*) and l^∞ (*b*)

The ED distribution was given using the NeQuick ionospheric model [17]:

vertical size of image element was 12.5 km;

horizontal size of image element was 50 km.

The rest of the parameters of the model were distributed by a uniform law:

solar activity index $F_{10.7} \in [63.7; 193]\cdot 10^{-22}$ $W\cdot m^{-2}\cdot Hz^{-1}$;

month $m \in [1; 12]$;

GMT time $t \in [0{:}00; 24{:}00]$ UTC;

geographic latitude (longitude of the ascending node of the orbit) $\lambda \in (0; 360]°$.

The spread in the parameters of the NeQuick model determines the spread in the errors of the initial approximation. The scale parameter σ was chosen taking into account the solar activity index $F_{10.7}$ ranging from 84 to 93 km.

The results of modeling by the algorithm for forming the initial approximation for the first case (10,000 simulations of the ED distribution were carried out) are shown in Fig. 3. The mean errors in this series of numerical experiments in the metrics l^2 and l^∞ are $\delta(l^2) = 0.23$ and $\delta(l^\infty) = 0.27$, respectively. This result is the upper estimate of the accuracy of the initial approximation among the three considered cases, since the parameters N_m and H_m were taken to be known a priori.

Fig. 4,*a* shows an example of one of 10,000 implementations of the ED distribution, formed by the NeQuick model for the following conditions:

solar activity index $F_{10.7} = 127.6 \cdot 10^{-22}$ $W\cdot m^{-2}\cdot Hz^{-1}$;

month: October

GMT $t = 10{:}00$;

geographic latitude (longitude of the ascending node of the orbit) $\lambda = 50°$.

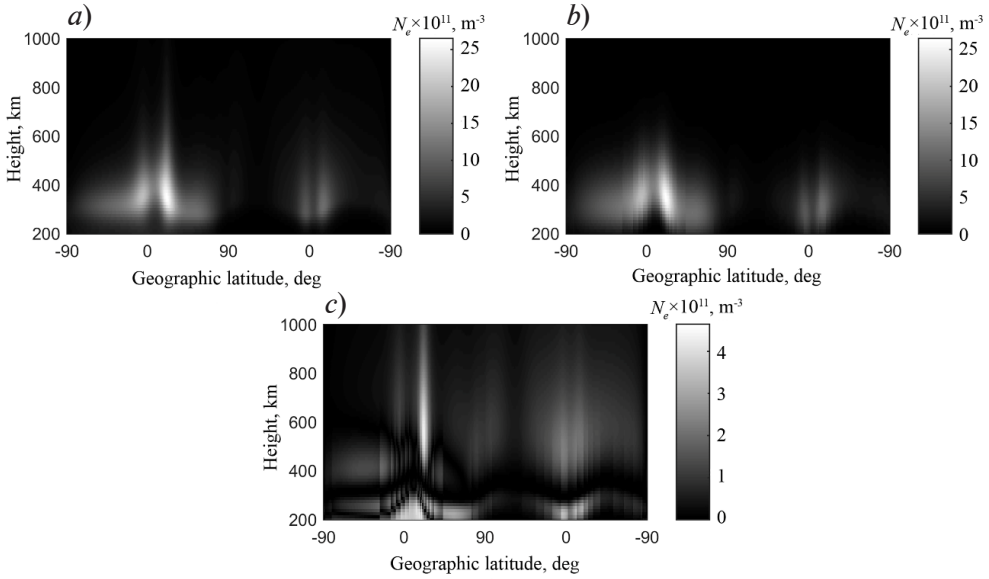

Fig. 4. Ionospheric ED distributions in the plane of the polar orbit in latitude-altitude coordinates: *a* is the model distribution; *b* is the initial approximation generated by Eq. (1) with the known N_m and H_m; *c* is the absolute value of the residual

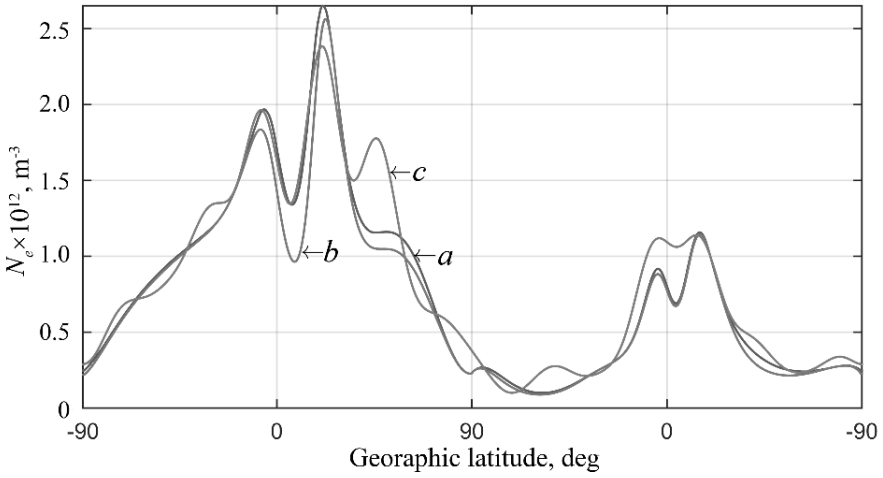

Fig. 5. Latitudinal ED profiles: initial $N_m(\varphi)_{H_m = H_m(\varphi)}$ (*a*); $N_m(\varphi)_{H_m = \langle H_m \rangle}$, taken for mean height (*b*); $\hat{N}_m(\varphi)$, calculated by Eq. (3) (*c*)

Figs. 4, *b*, *c* show the initial approximation formed for case I, and the absolute value of the residual between the model and the distribution generated for this implementation.

The latitudinal ED profile $\hat{N}_m(\varphi)$ was estimated in the simulation for cases II and III (see above) using Eq. (3) (Fig. 5,*c*) for the model distribution (Fig. 4,*a*). The value of the regularization parameter α in Eq. (3) was selected based on the minimization criterion for the residual:

$$d = \left\| \hat{N}_{m\,\alpha} - N_m \right\|_1 \to \min.$$

For comparison, Fig. 5,*a* shows the initial latitudinal profile $N_m(\varphi)_{H_m = H_m(\varphi)}$ of the model distribution, and Fig. 5,*b* the latitudinal profile of the model distribution for the mean height $N_m(\varphi)_{H_m = \langle H_m \rangle}$.

The difference between the profile in Fig. 5,*a* and the profiles in Figs. 5, *b*, *c* in the metrics l^2 and l^∞ is given in Table 1. It can be seen from the results obtained that the values of the latitudinal profile $N_m(\varphi)_{H_m = \langle H_m \rangle}$ for the mean height $\langle H_m \rangle$ can be used as values for the latitudinal profile $N_m(\varphi)_{H_m = H_m(\varphi)}$. This is used to generate the initial approximation for case III, where the values of $\hat{N}_m(\varphi)$ are given at a priori known heights H_m.

The solar activity index $F_{10.7}$ determines the shape of the ED profile and the height of the maximum in it [15]; therefore, the mean height of the ED maximum can be approximately described by a linear dependence

$$\langle H_m \rangle (F_{10.7}) = a \cdot F_{10.7} + b \pm \Delta \langle H_m \rangle,$$

where $a = 0.65 \cdot 10^{16}$ km$^3 \cdot$ Hz$^{-1} \cdot$ W^{-1}; $b = 243.4$ km; $\Delta\langle H_m \rangle = 18.7$ km is the spread in mean height depending on seasonal and diurnal effects for $P = 0.95$.

Table 1

Comparison of deviations δ of latitudinal profiles (in two metrics) from true latitudinal profile, obtained by two methods

Metric	Error δ	
	$N_m(\varphi)_{H_m = \langle H_m \rangle}$	$\hat{N}_m(\varphi)$
l^2	0.10	0.16
l^∞	0.19	0.23

Notations: $N_m(\varphi)_{H_m = \langle H_m \rangle}$, $\hat{N}_m(\varphi)$ are the latitudinal profiles: taken for the mean height and calculated by Eq. (3). The true latitudinal profile is $N_m(\varphi)_{H_m = H_m(\varphi)}$.

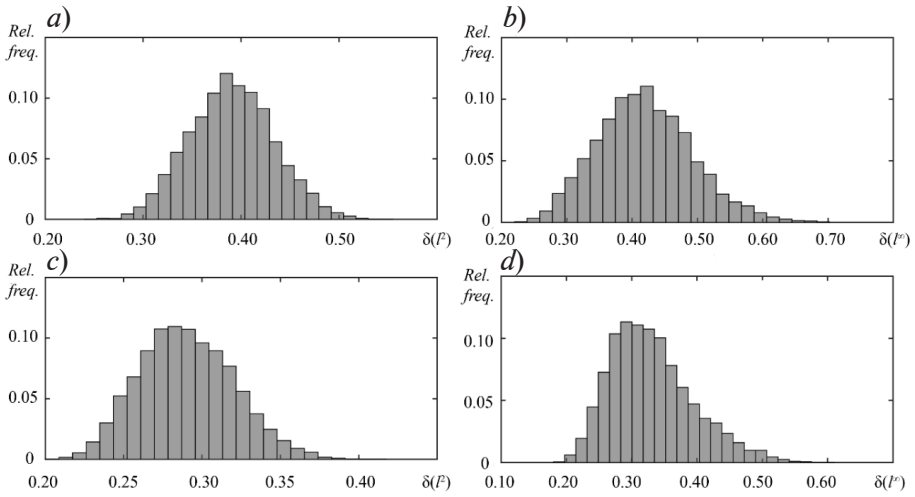

Fig. 6. Histograms of errors of initial approximation in metrics l^2 (*a*) and l^∞ (*b*) for case II,and l^2 (*c*) и l^∞ (*d*) for case III

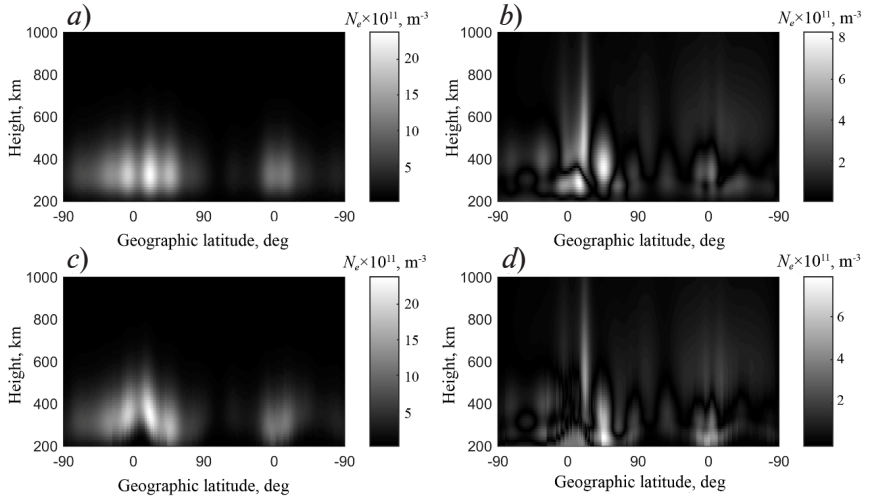

Fig. 7. Distributions of ionospheric ED in the plane of the polar orbit in latitude-altitude coordinates, obtained in the initial approximations by Eq. (4) for two values of the height: mean $\langle H_m \rangle$ (*a*) and known a priori H_m (*c*); the corresponding absolute values of the residuals are also given for cases with $\langle H_m \rangle$ (*b*) and H_m (*d*)

Table 2

Errors in generating the initial approximation in two metrics for the three considered cases for model distribution (see Fig. 4,*a*)

Metric	Error δ		
	N_m and H_m are known	$N_m = \hat{N}_m(\varphi)$, H_m is known	$N_m = \hat{N}_m(\varphi)$, $H_m = \langle H_m \rangle$
l^2	0.18	0.31	0.30
l^∞	0.18	0.30	0.25

If the seasonal and diurnal effects in the ionosphere are not taken into account, then the term $\Delta\langle H_m\rangle$ can be discarded, defining $\langle H_m\rangle$ in the second version of the algorithm as $\langle H_m\rangle = a \cdot F_{10.7} + b$.

Fig. 6 shows histograms for the distribution of errors in the initial approximation in the metrics l^2 and l^∞, generated for cases II and III for 10,000 numerical experiments. Fig. 7 shows the generated initial approximation and the absolute value of the residual between the model and the generated distributions for cases II and III for the implementation in Fig. 4,*a*.

Table 2 shows the errors in the initial approximation for the three considered cases of the model distribution (see Fig. 4,*a*). Cases II and III yield approximately the same accuracy, despite a noticeable visual difference (see Figs. 7, *a*, *c*).

According to the results of statistical modeling (Fig. 6), case II has mean errors of the initial approximation $\delta(l^2) = 0.39$ and $\delta(l^\infty) = 0.42$. The accuracy achieved is sufficient for obtaining a satisfactory solution to the tomographic problem, where the errors do not exceed the errors for the initial approximation [13] taken as a constant (the accuracy of the solution to the tomographic problem $\delta(l^2) = 0.35$ and $\delta(l^\infty) = 0.40$ for a reconstruction step of 50 km with respect to altitude). The accuracy of the initial approximation is higher for case III than for case II: $\delta(l^2) = 0.29$ and $\delta(l^\infty) = 0.33$, making this case similar to the initial approximation formed by the IRI-2007 model in [13] for obtaining the integral characteristics by transceiver devices of a constellation of satellites. Both versions of the algorithm (cases II and III) for generating the initial approximation are fast and can be implemented on board the satellite.

Reconstruction of ionospheric ED distribution. The quality with which the initial approximation was generated was assessed by tomographic reconstruction of the ED distribution using the approach proposed in [2, 3]. The configuration of satellites in low orbit, described in [3], was used as a scheme for detecting TEC: three satellites with transmitters and two with receivers, whose radio paths cover

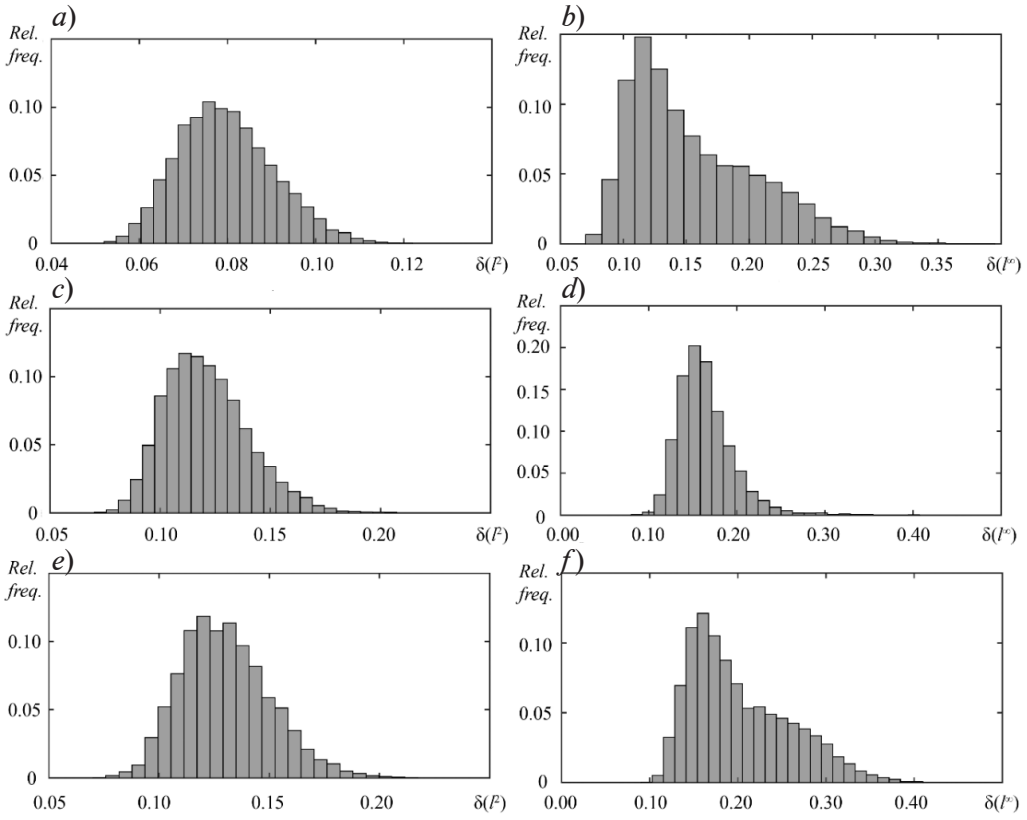

Fig. 8. Histograms for errors in reconstructing the ED profile for three cases of initial approximation in two metrics: l^2 (*a*, *c*, *e*) and l^∞ (*b*, *d*, *f*); cases I (*a*, *b*), II (*c*, *d*), III (*e*, *f*) were considered (see explanations in the text)

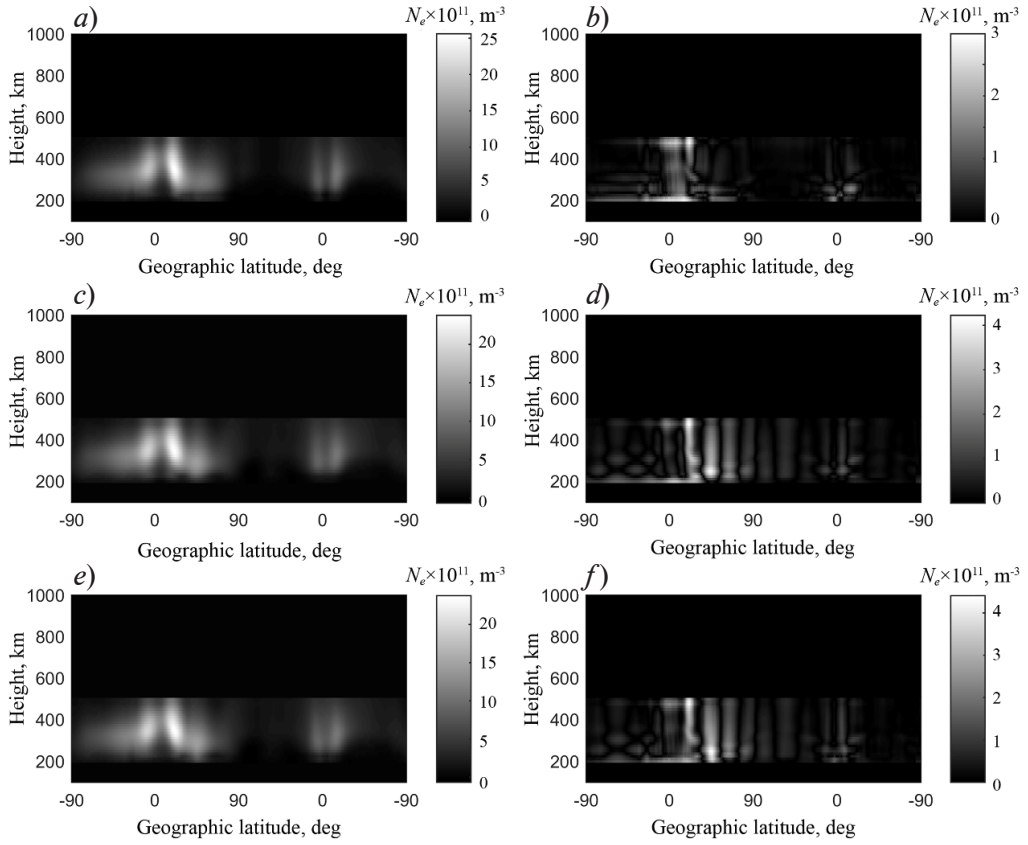

Fig. 9. Reconstruction of ionospheric ED distribution in the plane of polar orbit in latitude-altitude coordinates for three cases of initial approximation: I (*a*), II (*c*), III (*e*); the corresponding absolute values of the residuals for cases I (*b*), II (*d*), III (*f*) are also given

the altitude range from 200 to 500 km with a step of 50 km. The tomography problem was solved in this altitude range.

Fig. 8 shows the histograms for the distribution of errors in the reconstruction of the ED profile in the metrics l^2 and l^∞, obtained for three cases of the initial approximation (Eqs. (2), (5), (6)) for 10,000 numerical experiments. Case I, when N_m and H_m are given a priori, yields the reconstruction result with the most accurate characteristics (see Fig. 8, *a*, *b*) among all three cases of the initial approximations based on the Chapman distribution. Fig. 9 shows the reconstructed ED distributions for cases II and III of of the initial approximation. Reconstruction errors $\delta(l^2)$ and $\delta(l^\infty)$ for the corresponding cases are given in Table 3.

It can be seen from Fig. 9, *c*, *d* and *e*, *f*, corresponding to Cases II ($N_m = \hat{N}_m(\varphi)$, $H_m = \langle H_m \rangle$) and III ($N_m = \hat{N}_m(\varphi)$, H_m is known) of

Table 3

Comparison of errors in reconstructing the ED profile in two metrics for the three considered cases of the initial approximation for model distribution (see Fig. 4,a)

Metric	Error δ		
	N_m and H_m are known	$N_m = \hat{N}_m(\varphi)$, H_m is known	$N_m = \hat{N}_m(\varphi)$, $H_m = \langle H_m \rangle$
l^2	0.08	0.13	0.12
l^∞	0.11	0.18	0.16

the initial approximation, that the reconstructions obtained have a similar form and differ only slightly by the number of artifacts; in this case, the errors are mainly due to the errors in reconstructing the latitudinal profile $\hat{N}_m(\varphi)$. In turn, the artifacts obtained at an altitude of 200 km are due to the systematic reconstruction error [2, 3]. The height of the ED maximum in Case II ($N_m = \hat{N}_m(\varphi)$, $H_m = \langle H_m \rangle$), H_m, was reconstructed with satisfactory accuracy, despite the assumption that $H_m = \langle H_m \rangle$, and for this reason, this method (Case II) is preferable to Case III ($N_m = \hat{N}_m(\varphi)$, H_m is known), primarily because the reconstruction errors in the initial approximation for this case are smaller (see Fig. 8, *c*–*f*).

Conclusion

We have developed a numerical algorithm for generating the initial approximation of the ED profile, using it to solve the problem of ionospheric radio tomography by a low-orbit satellite constellation. The initial approximation generated by the algorithm is based on the Chapman distribution and is represented as a product of two factors responsible for the latitude and height distributions.

We have obtained an approximate analytical dependence of the latitudinal ED profile on the measured TEC data for an intersatellite detection scheme in the plane of the polar orbit.

We have confirmed that the latitudinal profile can be assessed by merely two satellites spaced apart in the orbit in such a way that the perigee altitude of their radio path is lower than the height of the ED maximum in the orbital profile.

We have found that the latitudinal distribution makes the greatest contribution to the final ED estimate.

Statistical modeling revealed that the errors in generating the initial approximation of the orbital ionospheric ED profile by TEC measurements, lie in the range from 20 to 55% in the metric l^2 (the errors in reconstructing the ED profile in the metric l^2 lie in the range from 8 to 20%), while the errors in generating the initial approximation by the NeQuick and IRI-2007 models reach 30% (the errors in reconstructing the ED profile in the metric l^2 lie in the range from 11 to 20%), and the errors in generating the initial approximation given by a constant value corresponding to the mean ED level reach 90% (the errors reconstructing the ED profile in the metric l^2 lie in the range from 35 to 40%).

The developed algorithm makes it possible to use real TEC measurements to generate the initial approximation, thus accounting for the short-term disturbances in the ionosphere, which are not directly accounted for with the NeQuick and IRI-2007 models.

In addition, the proposed algorithm has a simpler mathematical implementation than these models and requires less input data, allowing to solve the problem of generating the initial approximation on board a satellite.

The study was carried out within the framework of the FSSS-2020-0018 project, financed from the state assignment means given to winners of competition of scientific laboratories of educational organizations of higher education under the authority of Ministry of Education and Science of the Russian Federation.

REFERENCES

1. **Kunitsyn V.E., Tereshchenko E.D., Andreeva E.S.,** Radiotomografiya ionosfery [Radiotomography of ionosphere], Fizmatlit, Moscow, 2007 (in Russian).

2. **Nikolaev P.N.,** Method for reconstruction ionospheric electron density under inter-satellite data registration scheme, Proceedings of the XV Young Scientists Conference "Fundamental and Applied Space Researches", Ed. A.M. Sadovski, IKI RAN, Moscow, April 11–13, 2018, (2018) 73–80 (in Russian).

3. **Filonin O.V., Nikolayev P.N.,** Convolution algorithm as the method for reconstruction of two-dimensional electron density distribution in the satellite constellation orbital plane, Journal of Instrument Engineering. 62 (5) (2019) 462–469.

4. **Austen J.R., Franke S.J., Liu C.H.,** Ionospheric imaging computerized tomography, Radio Science. 23 (3) (1988) 299–307.

5. **Afraymovich E.L., Pirog O.M., Terekhov A.I.,** Diagnostics of large-scale structures of the high-latitude ionosphere based on tomographic signal processing of navigation satellites and data of ionospheric stations, Preprint of Siberian Institute of Terrestrial Magnetism, Ionosphere and Radio Wave Propagation, 1989.

6. **Romanov A.A., Trusov S.V., Adzhalova A.V., et al.,** Method of monitoring vertical distribution of ionospheric electron concentration, Pat. No. 2445652; Russian Federation, MPK G01V 3/12 (2006.01) G01S 13/95 (2006.01); Otkrytoe aktsionernoe obshchestvo "Rossijskaja korporatsija

raketno-kosmicheskogo priborostroenija i informatsionnykh sistem" (OAO "Rossijskie kosmicheskie sistemy") (RU) is a declarant and patentee. No. 2010126414/28, publ. 20.03.2012, Bull. No. 8.

7. **Romanov A.A., Trusov S.V., Novikov A.V., et al.,** Reconstruction of the two-dimensional distribution of the electron concentration of the ionosphere in the orbital plane of low-orbit satellite based on the analysis of the characteristics of coherent radiation, Electromechanical Matters, VNIIEM Studies, Moscow. 111 (2009) 37–42 (in Russian).

8. **Raymund T. D., Austen J.R., Franke S.J., et al.,** Application of computerized tomography to the investigation of ionospheric structures, Radio Science. 25 (5) (1990) 771–789.

9. **Heaton J.A., Jones G.O., Kersley L.,** Toward ionospheric tomography in place antarctica: first steps and comparison with dynasonde observations, Antarctic Science. 8 (3) (1996) 297–302.

10. **Mitchell C.N., Kersley L., Heaton J.A.T., Pryse S.E.,** Determination of the vertical electron-density profile in ionospheric tomography: experimental results, Annales Geophysicae. 15 (6) (1997) 747–752.

11. **Tereshchenko E.D., Khudukon B.Z., Romanova N.Y., et al.,** Radiotomographic observations of the ionosphere electron density at the Spitsbergen Archipelago-Kola Peninsula-Karelia meridian, Journal of Experimental and Theoretical Physics Letters, 78 (11) (2003) 707–708.

12. **Romanov A.A., Trusov S.V., Romanov A.A.,** Automated information technology for ionosphere monitoring on the low-orbit navigation satellite signals, Proceedings of the 4-th PICES Workshop on the Okhotsk Sea and Adjacent Areas (August 27–29, 2008, Abashiri, Japan). 203–207.

13. **Romanov A.A., Romanov A.A., Trusov S.V., Urlichich Yu.M.,** Sputnikovaya radiotomografiya ionosfery [Satellite radio tomography of the ionosphere], Moscow, Fizmatlit, 2013.

14. International Reference Ionosphere, http://irimodel.org. Accessed July 17, 2019.

15. **Zolesi B., Cander L.R.,** Ionospheric prediction and forecasting, Springer-Verlag, Berlin, Heidelberg, 2014.

16. **Wen W., Kalkan E.,** System identification based on deconvolution and cross correlation an application to a 20-story instrumented building in Anchorage, Alaska, Bulletin of the Seismological Society of America. 107 (2) (2017) 718–740.

17. **Giovanni G.Di, Radicella S.M.,** An analytical model of the electron density profile in the ionosphere, Advances in Space Research. 10 (11) 27–30.

Received 17.07.2019, accepted 27.07.2020.

THE AUTHOR

NIKOLAEV Petr N.
Samara National Research University
34 Moskovskoye Ave., Samara, 443086, Russian Federation
nikolaev.pn@ssau.ru

СПИСОК ЛИТЕРАТУРЫ

1. **Куницын В.Е., Терещенко Е.Д., Андреева Е.С.** Радиотомография ионосферы. М.: Физматлит, 2007. 336 с.

2. **Николаев П.Н.** Метод реконструкции электронной концентрации в ионосфере по схеме регистрации данных спутник-спутник // 15-я Конференция молодых ученых «Фундаментальные и прикладные космические исследования». Сб. трудов. Под ред. А.М. Садовского. Сер. «Механика, управление и информатика». М.: ИКИ РАН, 2018. С. 73–80.

3. **Филонин О.В., Николаев П.Н.** Алгоритм свертки как метод восстановления двумерного распределения электронной концентрации ионосферы в плоскости орбиты группировки спутников // Известия вузов. Приборостроение. 2019. Т. 62. № 5. С. 462–469.

4. **Austen J.R., Franke S.J., Liu C.H.** Ionospheric imaging computerized tomography // Radio Science. 1988. Vol. 23. No. 3. Pp. 299–307.

5. **Афраймович Э.Л., Пирог О.М., Терехов А.И.** Диагностика крупномасштабных структур высокоширотной ионосферы на основе томографической обработки сигналов навигационных ИСЗ и данных ионосферных станций. Препринт СибИЗМИР СО АН СССР, 1989. 18 с.

6. **Романов А.А., Трусов С.В., Аджалова А.В., Романов А.А., Урличич Ю.М.** Способ мониторинга вертикального распределения электронной концентрации ионосферы. Патент РФ № 2445652; опубл. 20.03.2012; бюлл. № 8.

7. **Романов А.А., Трусов С.В., Новиков А.В., Аджалова А.В., Романов А.А., Селин В.А.** Восстановление двумерного распределения электронной концентрации ионосферы в плоскости орбиты низкоорбитальных ИСЗ на основе анализа характеристик когерентного излучения // Вопросы электромеханики. Труды НПП ВНИИЭМ. М.: ФГУП «НПП ВНИИЭМ», 2009. Т. 111. С. 42–37.

8. **Raymund T. D., Austen J.R., Franke S.J., Lin C.H., Klobuchar J.A., Sralker J.** Application of computerized tomography to the investigation of ionospheric structures // Radio Science. 1990. Vol. 25. No. 5. Pp. 771–789.

9. **Heaton J.A., Jones G.O., Kersley L.** Toward ionospheric tomography in place antarctica: first steps and comparison with dynasonde observations // Antarctic Science. 1996. Vol. 8. No. 3. Pp. 297–302.

10. **Mitchell C.N., Kersley L., Heaton J.A.T., Pryse S.E.** Determination of the vertical electron-density profile in ionospheric tomography: experimental results // Annales Geophysicae. 1997. Vol. 15. No. 6. Pp. 747–752.

11. **Терещенко Е.Д., Худукон Б.З., Романова Н.Ю., Галахов А.А., Мельниченко Ю.А., Сухоруков В.М.** Радиотомографические наблюдения электронной плотности ионосферы на меридиане архипелаг Шпицберген – Кольский полуостров – Карелия // Письма в ЖЭТФ. 2003. Т. 78, № 11. С. 1221–1222.

12. **Romanov A.A., Trusov S.V., Romanov A.A.** Automated information technology for ionosphere monitoring on the low-orbit navigation satellite signals // The 4-th PICES Workshop on the Okhotsk Sea and Adjacent Areas (August 27–29, 2008, Abashiri, Japan). Pp. 203–207

13. **Романов А.А., Романов А.А., Трусов С.В., Урличич Ю.М.** Спутниковая радиотомография ионосферы. М.: Физматлит, 2013. 296 с.

14. International Reference Ionosphere. Режим доступа: http://irimodel.org (Дата обращения 17.07.2019).

15. **Zolesi B., Cander L.R.** Ionospheric prediction and forecasting. Berlin, Heidelberg: Springer-Verlag, 2014. 240 p.

16. **Wen W., Kalkan E.** System identification based on deconvolution and cross correlation an application to a 20-story instrumented building in Anchorage, Alaska // Bulletin of the Seismological Society of America. 2017. Vol. 107. No. 2. Pp. 718–740.

17. **Giovanni G.Di, Radicella S.M.** An analytical model of the electron density profile in the ionosphere // Advances in Space Research. 1990. Vol. 10. No. 11. Pp. 27–30.

Статья поступила в редакцию 17.07.2019, принята к публикации 27.07.2020.

СВЕДЕНИЯ ОБ АВТОРЕ

НИКОЛАЕВ Петр Николаевич – *кандидат физико-математических наук, ассистент межвузовской кафедры космических исследований Самарского национального исследовательского университета имени академика С.П. Королева, г. Самара, Российская Федерация.*

443086. Российская Федерация, г. Самара, Московское шоссе, 34

nikolaev.pn@ssau.ru